Journal of the European Ceramic Society **10** (1992) 95–100

Processing of Alumina/Nickel Composites

W. H. Tuan

Institute of Materials Engineering, National Taiwan University, Taipei, Taiwan

&

R. J. Brook

Max-Planck-Institut für Metallforschung, D-7000 Stuttgart, FRG

(Received 20 November 1990; revised version received 15 November 1991; accepted 2 December 1991)

Abstract

Brittle solids can be toughened by introducing ductile inclusions. In the present study, nickel inclusions are incorporated into an alumina matrix. Three processing routes are investigated, namely (1) a powder metallurgy route, (2) a gas reduction route, and (3) a reaction sintering route. Optimal processing conditions for each route are explored. The properties of the resulting composites are measured and compared in the light of the respective routes and microstructures.

Eine Zähigkeitssteigerung bei spröden Werkstoffen kann durch das Einbringen duktiler Einschlüsse erreicht werden. In der vorliegenden Arbeit wurden Nickel-Einschlüsse in eine Aluminiumoxid-Matrix eingelagert. Es wurden drei verschiedene Herstellungsmethoden untersucht, und zwar erstens ein pulvermetallurgischer Prozess, zweitens ein Prozess über Gasreduktion und drittens die Herstellung über Reaktionssintern. Die optimalen Herstellungsbedingungen für jede der genannten Herstellungsmethoden wurden erarbeitet. Die Eigenschaften der sich ergebenden Verbundwerkstoffe wurden bestimmt und unter dem Aspekt des Herstellungsprozesses und der Gefüge miteinander verglichen.

Des solides fragiles peuvent être renforcés en introduisant des inclusions ductiles. Dans cette présente étude, des inclusions de nickel sont incorporées dans une matrice d'alumine. Trois procédés différents sont étudiés: (1) un procédé par mélange de poudres métalliques, (2) un procédé de réduction en phase gazeuse, et (3) un procédé de réaction par frittage. Pour chaque procédé les conditions expérimentales optimales sont recherchées. Les propriétés des composites obtenus sont mesurées et comparées à la lumière des procédés respectifs et des microstructures.

1 Introduction

The application of ceramics as engineering parts is handicapped by their brittleness. By the incorporation of metallic reinforcements, the fracture toughness of ceramics is improved significantly (Table 1).[1–14] The toughness enhancement is attributed to the plastic work expended upon deforming the ductile inclusions. In order for the plastic deformation to be fully exploited, two conditions have to be fulfilled: firstly, to ensure that the crack is attracted by the metallic particle, the elastic modulus of the metal should be lower than that of the ceramic matrix; secondly, the metallic particles need to be bonded to the brittle matrix, which means that they should be kept below the critical size at which stresses arising from any thermal expansion mismatch become sufficient to induce cracks.

Theoretical work[15,16] suggests that the toughness enhancement is increased with increase in inclusion volume fraction, yield strength and diameter. Recent experimental work[16,17] shows that a degree of debonding at the ceramic/metal interface will increase the extent of plastic work. The degree of debonding strongly depends on the characteristics of the interface, which are in turn determined by the processing route used.

From Table 1, it can be seen that most metal-reinforced ceramic composites have been formed by powders are thoroughly mixed before consolidation. powder methods, namely ceramic and metallic The consolidation processes include the liquid-

Journal of the European Ceramic Society 0955-2219/92/$05.00

Table 1. The reported values of toughness for various ceramic/metal composites. $K_{IC,c}/K_{IC,o}$ is the ratio of the fracture toughness of composite to that of matrix

Systems	*Fabrication method*	$K_{IC,c}/K_{IC,o}$	*Comments*	*References*
Al_2O_3/Mo	P/M + hot-pressing	1·2	5 v/o	1
Al_2O_3/Mo fibre	P/M + hot-pressing	16	12 v/o, strong bonding	2
NaCl/Au	Electrodiffusion	10	Non-bonded	3
MgO/Fe, Ni	Reduction in H_2	1·2	2 v/o, weak bonding	4
MgO/Fe, Ni, Co	P/M + hot-pressing	3	40 v/o, weak bonding	4
MgO/Ni fibre	P/M + hot-pressing	10	33 v/o, weak bonding	4
$Al_2O_3/Fe_{0·8}Cr_{0·2}$	Selective reduction + hot-pressing	1·8	20 w/o	5
WC/Co	P/M	2	Strong bonding	6
Glass/Ni	P/M + hot-pressing	1·2	20 v/o, non-bonded	7
Glass/Ni	P/M + hot-pressing	1·2	10 v/o, non-bonded	8
Glass/Al	P/M + hot-pressing	8	20 v/o, strong bonding	9
TiB_2/Ni	P/M + hot-pressing	1·1	1·4 w/o	10
Glass/Fe–Al–Co	P/M + hot-pressing	1·7	10 v/o	11
Al_2O_3/Al	Lanxide process	2·8	Room temperature	12
OH-Ap/Ni-alloy	P/M + hot-pressing	6	Hastelloy fibre, 30 v/o	13
OH-Ap/Fe-alloy	P/M + hot-pressing	7	FeCralloy fibre, 30 v/o	13
Al_2O_3/Ni	Selective reduction	2	13 v/o	14

P/M = Powder metallurgy route.

phase sintering of a ceramic powder with a molten metal,[6] the hot-pressing of ceramic/metal powder mixtures,[1,2,5,7–11,13] and the reduction of a metallic oxide to form the metallic phase at grain junctions.[4,14] Two difficulties arise from the liquid-phase sintering process: firstly, the wetting of the ceramic by the metallic melt is usually poor,[18] which results in low density; hot-pressing is therefore needed; secondly, the metallic particles need to be firmly bonded to the brittle matrix (below a critical size) to ensure that they are deformed as the matrix crack extends; however, the plasticity of the metal makes it difficult to achieve fine particles by milling. These difficulties can be overcome by a selective reduction process,[14] in which two oxide powders are mixed and subsequently reduced into an oxide and a metallic phase. Composites containing metallic inclusions with a size around one micrometer have been prepared by this method. The toughness of such a composite containing 13 v/o metallic inclusions can be twice that of the matrix alone.[14]

A less conventional method, the dimox (directed metal oxidation) process is available for forming metal-reinforced ceramic composites.[19,20] This method involves the reaction of a molten metal with the surrounding atmosphere. For example, alumina/aluminium composites are prepared by directed oxidation of an aluminium melt. The reaction product, e.g. alumina, is formed as a continuous phase; the unreacted reactant, e.g. aluminium, is found in channels within the reaction layer. The reported value for the toughness of the composite containing 20 v/o aluminium is 2·8 times that of alumina alone.[12]

In the present study, nickel inclusions are introduced into an alumina matrix by three different processing routes: (1) a powder metallurgy route, in which the metal and ceramic powders are mixed and subsequently sintered; (2) a gas reduction route, in which a nickel aluminate spinel is reduced in a reducing atmosphere to form an alumina/nickel composite; (3) a reaction sintering route, in which alumina/nickel composites result from the reaction between aluminium and nickel oxide. The optimal processing conditions for each route are explored and the three routes are compared in terms of their suitability for composite formation.

2 Experimental

2.1 Powder metallurgy route

The flow diagram of the process is shown in Fig. 1(a). Alumina powders (1, XA1000SG, mean size: 0·59 μm, The Aluminum Co. of America, USA; 2, F500, abrasive alumina, 16 μm, H. C. Starck, Berlin, FRG) and 25·2 w/o nickel powder (14·2 μm, E. Merck AG, Darmstadt, FRG) were attrition milled for 4 h with isopropanol and alumina balls as grinding media. The addition of nickel particles represented 13 v/o inclusion phase for the fully dense composite. The particle size distribution was determined before and after milling (Granulometer HR 850, Cilas-Alcatel Co., France). The powder pellets of 2 cm in diameter and 0·5 cm in height were formed by cold isostatic pressing (CIP) at 200 MPa. The sintering was performed in a box furnace at temperatures between 1400°C and 1700°C for 1 h.

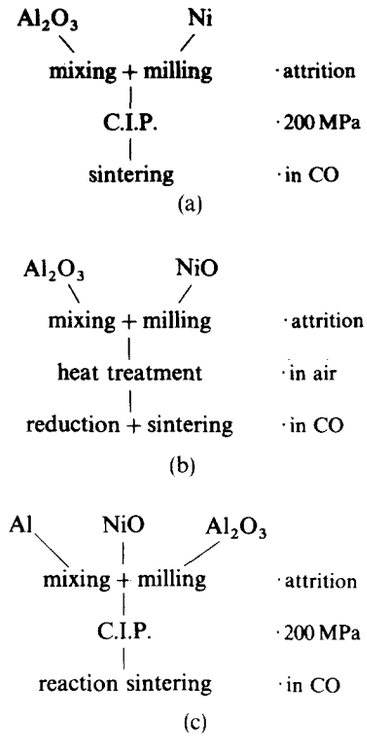

Fig. 1. The flow diagrams for the processing routes investigated in the present study: (a) powder metallurgy route, (b) gas reduction route, and (c) reaction sintering route.

The heating and cooling rates were 5°C/min. A graphite powder bed surrounded the powder compacts to generate a reducing atmosphere at the sintering temperature used.

2.2 Gas reduction route

The flow diagram of the process is shown in Fig. 1(b). Alumina (XA1000SG) and 30 w/o nickel oxide (Alfa product, 16·5 μm, Johnson Matthey Co., Denver, USA) were attrition milled. The preparation procedures for the powder compacts were the same as those for the powder metallurgy route. The powder compacts were heat treated in air at 1600°C for 1 h, or at 1600°C for 10 h, or at 1300°C for 10 h. The compacts were then sintered in a reducing atmosphere for 1 h at 1600°C or 1700°C. Some un-heat-treated powder compacts were also sintered at the same time.

2.3 Reaction sintering route

The process (Fig. 1(c)) started from powder mixtures of 56·6 w/o alumina (F500), 14·4 w/o aluminium droplets (ECKA AS081, around 50 μm in length and around 20 μm in diameter, Eckart-Werke, Fuerth, FRG) and 29·0 w/o nickel oxide. The reaction,

$$2Al + 3NiO = Al_2O_3 + 3Ni \qquad (1)$$

took place during firing.

Polished surfaces were prepared by cutting the samples along the axial direction of the discs and by polishing with diamond paste to 1 μm. The inclusion size of the nickel was determined by the linear intercept technique. Indentation was performed on a Zwick microhardness tester with a Vickers diamond indenter and a 50 N load. The relationship proposed by Lawn *et al.*[20] was used to calculate the values of K_{IC}. Toughness measurements were performed on specimens with a relative density higher than 94% theoretical density.

3 Results

3.1 Powder metallurgy route

When the nickel particles are milled together with fine alumina powder (XA1000SG), the particle size of the nickel is unaffected by the milling process. The relative densities of the compacts containing 0 and 25 w/o nickel are shown in Fig. 2 as a function of sintering temperature. The microstructures of the composites sintered at 1500°C, 1600°C and 1700°C for 1 h are shown in Fig. 3(a), (b) and (c) respectively. The nickel inclusions exhibit a bimodal size distribution. The coarse nickel inclusions result from the ineffective milling. The nickel inclusions become more spherical as the sintering temperature is increased, demonstrating the poor wetting between alumina and a nickel melt.

Abrasive alumina alone is milled down to 0·78 μm after attrition. Nickel particles are milled down to about 1 μm when milled in the presence of coarse alumina particles.[21] The microstructure of the composite is shown in Fig. 4. The bimodal size

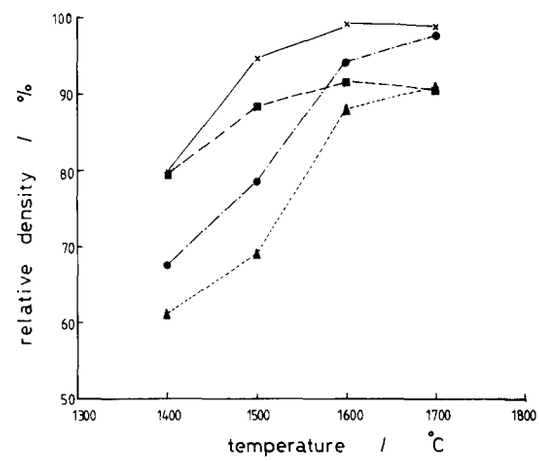

Fig. 2. The density of the composites as a function of sintering temperature. The composites are prepared by the powder metallurgy route and sintered at the indicated temperature for 1 h. ×, XA1000SG; ■, XA1000SG + Ni; ●, F500; ▲, F500 + Ni.

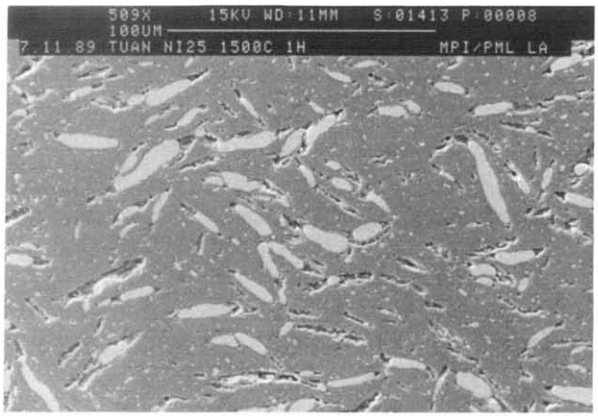

(a)

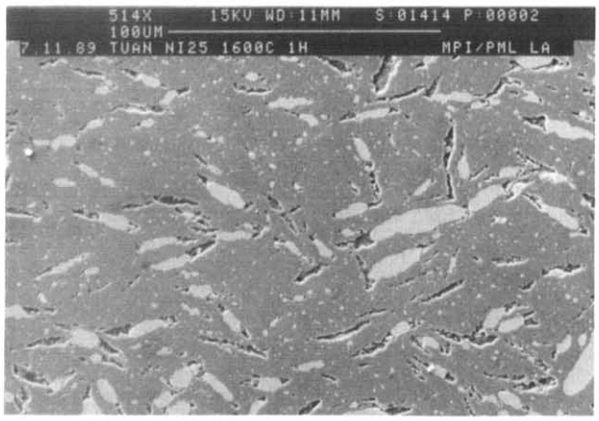

(b)

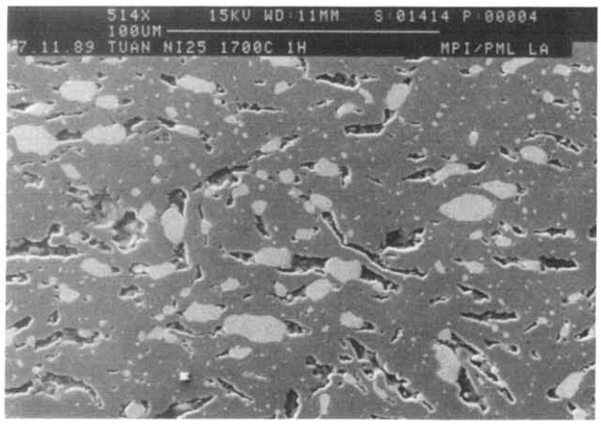

(c)

Fig. 3. Polished sections for the composites prepared by the powder metallurgy route. Sintering temperature: (a) 1500°C; (b) 1600°C; (c) 1700°C.

distribution of the nickel inclusions can no longer be observed; the mean inclusion size after sintering is 2·3 μm. The densities of the composites and of the standard alumina compacts are also shown in Fig. 2. Although the standard alumina compact can be sintered to above 97% theoretical density, the density of the composites is significantly decreased due to the presence of the nickel inclusions.

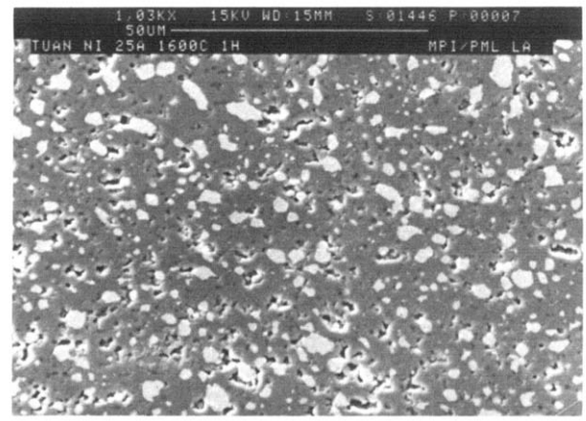

Fig. 4. Polished section for the composite prepared from the coarse alumina and nickel mixtures.

3.2 Gas reduction route

The mean particle size of the powder mixtures of alumina and nickel oxide after attrition milling is below 0·5 μm. The X-ray results show that nickel aluminate spinel results from the heat treatment; only alumina and nickel are present for the specimens sintered in a reducing atmosphere above 1500°C. The relative density, inclusion size of the nickel and toughness of the composites prepared by this process are shown in Table 2. With the exception of the density of the specimen heat treated at 1600°C in air for 10 h and sintered at 1600°C (90% theoretical density), the densities of other specimens are all above 95%. Typical microstructures are shown in Fig. 5. The composite containing 13 v/o nickel has been heat treated at 1600°C in air for 1 h, being sintered subsequently at 1600°C for 1 h.

3.3 Reaction sintering route

Aluminium particles are milled down to about 1 μm by being comminuted together with coarse alumina particles.[21] The relative density, inclusion size and fracture toughness of the composites are shown in Table 3. The density of the composite sintered at

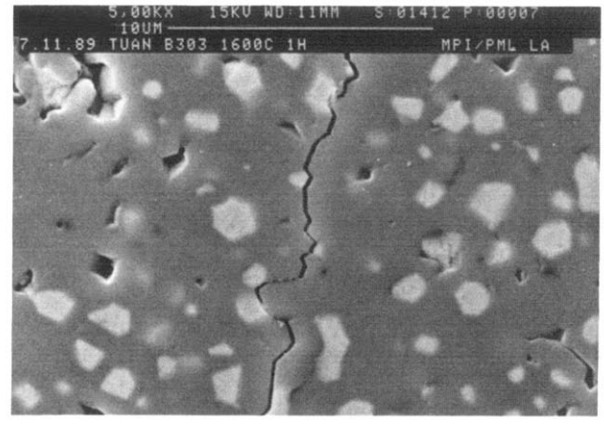

Fig. 5. Polished section for the composite prepared by the gas reduction route.

Table 2. The relative density, inclusion size, fracture toughness and toughness ratio for the composites prepared by the gas reduction route. The density after heat treatment in air is denoted as starting density. The volume fraction of nickel for all the composites is 0·13. 2·7 MPa $m^{1/2}$ is used as the fracture toughness for alumina

	Heat treatment			
	None	*1600°C/1 h*	*1600°C/10 h*	*1300°C/1 h*
Starting density (%td)	53	70	80	50
Sintering condition (1600°C/1 h)				
Final density (%td)	97	96	90	98
Inclusion size (μm)	1·3	1·6	2·4	1·5
Toughness (MPa$\sqrt{m}$)	4·0	4·9	—	4·8
Toughness ratio	1·5	1·8	—	1·8
Sintering condition (1700°C/1 h)				
Final density (%td)	97	96	96	95
Inclusion size (μm)	3·9	2·4	3·2	3·4
Toughness (MPa$\sqrt{m}$)	4·4	4·9	5·0	4·4
Toughness ratio	1·6	1·8	1·9	1·6

1600°C and 1700°C is higher than 95% theoretical density.

A fracture surface is shown in Fig. 6(a), tilted during observation to reveal the strained nickel particles. The particles can also be observed on a polished surface (Fig. 6(b)) where the crack on the polished surface has been introduced by indentation.

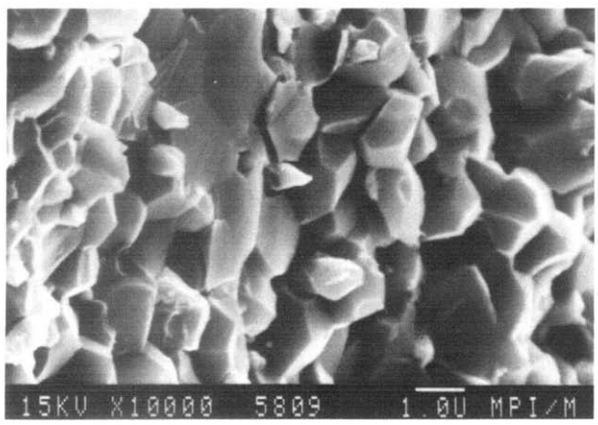

(a)

(b)

Fig. 6. Microstructures for the composite prepared by the reaction sintering route.

Table 3. The relative density, inclusion size, fracture toughness and toughness ratio for the composites prepared by the reaction sintering. The volume fraction of nickel is 0·11

	Sintering condition	
	1600°C/1 h	*1700°C/1 h*
Final density (% td)	96	98
Inclusion size (μm)	1·3	1·6
Toughness (MPa$\sqrt{m}$)	3·6	3·6
Toughness ratio	1·3	1·3

4 Discussion

Powder mixtures of alumina and nickel are difficult to sinter without pressure to above 90% theoretical density, despite the fact that the particle size of the nickel can be decreased to the submicron range. One factor is the poor wetting between alumina and a nickel melt (Fig. 2). For the composites prepared by gas reduction or reaction sintering, densities above 90% theoretical density can be achieved by pressureless sintering above 1600°C. The poor wetting between the ceramic and the metal melt can be improved by a suitable reaction at the interface.[22] For the present system, both the reduction and the chemical reactions are found to be beneficial.

For the particulate composite-containing phases with different thermal expansion coefficients, internal stresses are set up within and around particles as the composite cools from the firing temperature. The particle/matrix interface is subjected to a radial tensile stress when the thermal expansion coefficient of the particle is bigger than that of the matrix as is the case for the Ni/Al_2O_3 system. The linear elastic solution for the tensile stress, σ_{th}, can be calculated by the relationship proposed by Selsing[23] as

$$\sigma_{th}[\Delta a\, \Delta T]/\{[(1+v_m]/2E_m] + [(1-2v_p)/E_p]\} \quad (2)$$

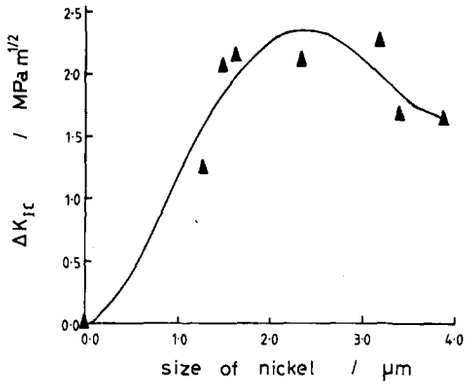

Fig. 7. The fracture toughness increase as a function of inclusion size. The composites are prepared by the gas reduction route.

where Δa is the difference in the two expansion coefficients, ΔT the cooling range over which the internal stress is no longer relaxed by the system (1400 K is assumed for the sintering condition used in the present study) and v and E the Poisson's ratio and the elastic modulus, respectively; subscripts m and p stand for matrix and particulate, respectively. By using $E_m = 380$ GPa, $E_p = 200$ GPa, $a_m = 9 \times 10^{-6}$, $a_p = 15 \times 10^{-6}$, and $v_m = v_p = v_p = 0{\cdot}25$, a value of 2·0 GPa is obtained.

By applying an energy balance concept, the critical particle size, d_c, can be calculated from the relationship[24,25]

$$d_c = [8K_{IC}^2]/\{(\sigma_{th})^2[(1+v_m)+2(E_m/E_p)(1-2v_p)\} \quad (3)$$

where K_{IC} is the fracture toughness of alumina; 2·7 MPa m$^{1/2}$ is used in the calculation.[14] A critical diameter, 4·5 μm, for the alumina/nickel composites is then obtained.

The fracture toughness of the composites prepared by the gas reduction route is shown in Fig. 7 as a function of inclusion size. When the size of the nickel is bigger than 2·5 μm, the toughness of the composites is reduced, suggesting a critical inclusion size of some 2·5 μm. The fact that the composites are not fully dense may cause the difference between the theoretical prediction and experimental results.

In microstructural observation, bridging nickel particles are observed behind the crack front consistent with a toughening mechanism involving plastic deformation of the metal particles.

References

1. Rankin, D. T., Stiglich, J. J., Petrak, D. R. & Ruh, R., Hot pressing and mechanical properties of Al_2O_3 with an Mo-dispersed phase. *J. Am. Ceram. Soc.*, **54** (1971) 277.
2. Simpson, L. A. & Wasylyshyn, A., Fracture energy of Al_2O_3 containing Mo-fibers. *J. Am. Ceram. Soc.*, **54** (1971) 56.
3. Forwood, C. T., The work of fracture in crystals of sodium chloride containing cavities. *Phil. Mag.*, **18** (1968) 657.
4. Hing, P. & Groves, G. W., The microstructure and fracture properties of MgO crystals containing a dispersed phase. *J. Mater. Sci.*, **7** (1972) 422; The strength and fracture toughness of polycrystalline magnesium oxide containing metallic particles and fibres. *J. Mater. Sci.*, **7** (1972) 427.
5. Devaux, X., Laurent, C., Brieu, M. & Rousset, A., Propriétés microstructurales et mécaniques de nanocomposites à matrice céramique. *C. R. Acad. Sci. Paris*, t. 312, Serie II (1991) p. 1425.
6. Chermant, L. J. & Osterstock, F., Fracture toughness and fracture of WC–Co composites. *J. Mater. Sci.*, **11** (1976) 1939.
7. Green, D. J., Nicholson, P. S. & Embury, J. D., Crack-particle interactions in brittle particulate composites. In *Ceramic Microstructure '76*, ed. R. M. Fulrath and J. A. Pask, Westview Press, Boulder, Colorado, 1977, p. 813.
8. Biswas, D. R., Strength and toughness of indented glass–nickel compacts. *J. Mater. Sci.*, **15** (1980) 1696.
9. Krstic, V. V. Nicholson, P. S. & Hoagland, R. G., Toughening of glasses by metallic particles. *J. Am. Ceram. Soc.*, **64** (1981) 499.
10. Ferber, M. K., Becher, P. F. & Finch, C. B., Effect of microstructure on the properties of TiB_2 ceramics. *J. Am. Ceram. Soc.*, **66** (1983) C-2.
11. Jessen, T. & Lewis III, D., Effect of crack velocity on crack resistance in brittle-matrix composites. *J. Am. Ceram. Soc.*, **72** (1989) 818.
12. Budiansky, B., Amazigo, J. C. & Evans, A. G. Small-scale crack bridging and the fracture toughness of particulate-reinforced ceramics. *J. Mech. Phys. Solids*, **36** (1988) 167.
13. de With, G. & Corbijn, A. J., Metal fibre reinforced hydroxy-apatite ceramics. *J. Mater. Sci.*, **24** (1989) 3411.
14. Tuan, W. H. & Brook, R. J., The toughening of alumina with nickel inclusions. *J. Eur. Ceram. Soc.*, **6** (1990) 31.
15. Sigl, L. S., Mataga, P. A., Dalgleish, B. J., McMeeking, R. M. & Evans, A. G., On the toughness of brittle materials reinforced with a ductile phase. *Acta Metall.*, **36** (1988) 945.
16. Ashby, M. F., Blunt, F. G. & Bannister, M., Flow characteristics of highly constrained metal wires. *Acta Metall.*, **37** (1989) 1847.
17. Flinn, B. D., Ruehle, M. & Evans, A. G., Toughening in composites of Al_2O_3 reinforced with Al. *Acta Metall.*, **37** (1989) 3001.
18. Humenik, Jr, M. & Kingery, W. D., Metal-Ceramic interactions: III, Surface tension and wettability of metal-ceramic systems. *J. Amer. Ceram. Soc.*, **37** (1954) 18.
19. Newkirk, M. S., Urqhart, A. W. & Zwicker, H. R., Formation of Lanxide ceramic composite materials. *J. Mater. Res.*, **1** (1986) 81.
20. Lawn, B. R., Evans, A. G. & Marshall, D. B., Elastic/plastic indentation damage in ceramics: the median/radial crack system. *J. Am. Ceram. Soc.*, **63** (1984) 574.
21. Claussen, N., Le, T. & Wu, S., Low shrinkage reaction-bonded alumina. *J. Eur. Ceram. Soc.*, **5** (1989) 29.
22. Halverson, D. C., Pyzik, A., Aksay, I. A. & Snowden, W. E., Processing of boron carbide–aluminum composites. *J. Am. Ceram. Soc.*, **72** (1989) 775.
23. Selsing, S., Internal stresses in ceramics. *J. Amer. Ceram. Soc.*, **44** (1961) 419.
24. Davidge, R. W. & Green, T. J., The strength of two-phase ceramic/glass materials. *J. Mater. Sci.*, **3** (1968) 629.
25. Magley, D. J., Winholtz, R. A. & Faber, K. T., Residual stresses in a two-phase microcracking ceramic. *J. Am. Ceram. Soc.*, **73** (1990) 1641.